The International Journal of Advanced Manufacturing Technology (2018) 99:1195–1201
https://doi.org/10.1007/s00170-018-2553-1

ORIGINAL ARTICLE

Detection of weak fault using sparse empirical wavelet transform for cyclic fault

Yanfei Lu[1] · Rui Xie[2] · Steven Y. Liang[1,3]

Received: 16 May 2018 / Accepted: 12 August 2018 / Published online: 17 August 2018

Abstract

The successful prediction of the remaining useful life of rolling element bearings depends on the capability of early fault detection. A critical step in fault diagnosis is to use the correct signal processing techniques to extract the fault signal. This paper proposes a newly developed diagnostic model using a sparse-based empirical wavelet transform (EWT) to enhance the fault signal to noise ratio. The unprocessed signal is first analyzed using the kurtogram to locate the fault frequency band and filter out the system noise. Then, the preprocessed signal is filtered using the EWT. The l_q-regularized sparse regression is implemented to obtain a sparse solution of the defect signal in the frequency domain. The proposed method demonstrates a significant improvement of the signal to noise ratio and is applicable for detection of cyclic fault, which includes the extraction of the fault signatures of bearings and gearboxes.

Keywords Ball bearing · Fault diagnosis · Sparse matrices · Wavelet transforms

1 Introduction

The most common component in rotating machineries is the rolling element bearing. Because of the commonality of using bearings to support load and maintain balance of the system, the prediction of the highly stochastic degradation patterns of bearings becomes a challenge that industries are encountering today. To address the stochastic nature of bearing failure, various maintenance schematics were proposed to accommodate the industry requirements. The accurate diagnosis of the location and defect severity of the bearing fault is critical to implement corresponding maintenance [1–3].

Randall and Antoni have proposed a general guide lines of bearing diagnosis in reference [4]. The initial stage includes using various techniques such as time-series model, adaptive line enhancer, and time synchronous average to separate the discrete frequency noise. However, these methods have several disadvantages. The parameters of the time-series model is non-stationary for the vibrational signal of bearings as indicated in reference [5]. Therefore, an adaptive algorithm is required in general [1]. Time synchronous average normally requires tachometer or similar device to be installed on the equipment [6]. The cost and added complexity could make the order tracking and time synchronous average inapplicable. Although various research claims order tracking can be implemented only with vibration signal [7–10], the condition is very limited, and it is not applicable for weak fault.

McFadden implemented the high-frequency resonance technique, also known as the envelope analysis, for fault detection of rolling element bearings [11]. This method extracts the bearing fault by examining the resonance generated by the impact of the fault site and is very effective in early fault detection [12]. Randall et al. established the relationship between the envelope analysis and the spectral correlation for cyclostationary machine signals [12]. This finding laid the foundation of the spectral analysis. Antoni proposed using the spectral kurtosis (SK) for analyzing non-stationary signals in reference [13]. The SK detects transients of vibrational signal regardless of presence of strong additive noise. Later, Antoni implemented the fast kurtogram in combination with envelope analysis for the extraction of fault frequency [14].

✉ Yanfei Lu
ylu318@gatech.edu

[1] George W. Woodruff School of Mechanical Engineering, Georgia Institute of Technology, Atlanta, GA 30332, USA

[2] Department of Statistics at the University of Georgia, Athens, GA 30602, USA

[3] College of Mechanical Engineering, Donghua University, Shanghai 201620, China

The model significantly reduces the computation of the traditional kurtogram [15] and improves the applicability for online monitoring.

The empirical mode decomposition (EMD) proposed by Huang et al. [16] is very effective for processing nonlinear and non-stationary signals in bearing diagnosis [17]. However, the lack of mathematical theory limits the method to be implemented in certain applications. Daubechies et al. proposed a model similar to the EMD to retrieve various modes of signal [18]. Although the EMD yields excellent results in processing nonlinear and non-stationary signals, the drawbacks of mode mixing, end effects, and lack of criteria for sifting have created issues in the fault extraction of bearings. To address this problem, Torres et al. proposed the complete ensemble empirical mode decomposition method to alleviate the mode mixing of the traditional EMD and improve the computation efficiency [19]. The empirical wavelet transform (EWT) developed by Gilles combined the advantages of the EMD and wavelet transform [20]. The EWT overcame the deficiency of dyadic subdivision of the traditional wavelet by making the wavelet adaptive. It is shown to be effective in fault diagnosis of wind turbine [21].

In this paper, a sparse-based bearing diagnosis model is proposed. The model uses the kurtogram and envelope analysis to preprocess the signal to remove undesirable system noise and improve signal to noise ratio in the desired frequency range. A sparse empirical wavelet is implemented to obtain a sparse frequency-domain representation of the early weak fault signal and its second harmonic. Experimental data is used to validate the diagnostic model. The proposed method significantly enhanced the ability of the extraction of the weak fault signature by enhancing the signal to noise ratio in comparison with the traditional EWT.

2 Diagnostic model

The proposed diagnostic model is shown in Fig. 1. The vibration signal of bearing is first analyzed using the kurtogram to location the resonance frequency and determine the bandwidth for the bandpass filter. A 100th-order AR filter is implemented to reduce the random noise in the system before performing the kurtogram. The segmentation of the signal in the frequency domain is obtained using a 1/3-binary tree of filter-banks to achieve better resolution on the frequency domain. The passband of the three additional quasi-analytic bandpass filter is [0,], $[\frac{1}{6}, \frac{1}{3}]$, and $[\frac{1}{3}, \frac{1}{2}]$, respectively. The resolution can be finely tuned by adding more bandpass filters with the increase of computation complexity. In this proposed model, a level of 7 is selected based on the 20,480-Hz sampling frequency to achieve a minimum resolution of 26.67 Hz in the kurtogram. The signal is filtered based on the information obtained from the kurtogram, and the envelope analysis is implemented to locate the fault frequency and obtain the processed envelope signal. The envelope signal is then filtered by the sparse EWT to obtain a sparse solution of the frequency-domain signal which contains the fault signature.

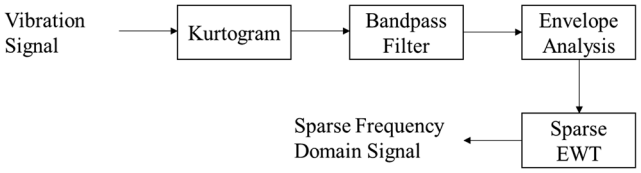

Fig. 1 Bearing diagnostic model

2.1 Kurtogram and envelope analysis

Spectral kurtosis is suited for bearing diagnosis because of its capability to detect weak transient signal in additive noise. The implementation of the SK assumes that the vibration signal of bearings can be presented in (1):

$$y(t) = x(t) + n(t) \tag{1}$$

where $y(t)$ is the measured vibration signal, $x(t)$is the fault signal with transients, and $n(t)$is the stationary system noise. The SK is normally defined as (2) [15]:

$$SK_X(f) = \frac{\left\langle |H(n,f)|^4 \right\rangle}{\left\langle |H(n,f)|^2 \right\rangle^2} - 2 \tag{2}$$

where $H(n,f)$ is the complex envelope of signal at frequency f and $\langle |H(n,f)|^4 \rangle$ is the temporary average of the envelope signal. The SK of a non-stationary signal is presented by (3) [15]:

$$SK_Y(f) = \frac{SK_X(f)}{[1 + SNR(f)]^2} \tag{3}$$

where $SK_Y(f)$ is the SK of the signal $y(t)$, $SK_X(f)$is the SK of the signal $x(t)$, and $SNR(f)$ is the signal to noise ratio. When the signal to noise ratio is high, $SK_Y(f)$ is approximately equivalent to $SK_X(f)$. When the signal to noise ratio is low, $SK_Y(f)$ approaches zero. Therefore, by searching the whole frequency-domain, the SK is capable of distinguishing the fault signal from system noise.

The fast kurtogram examines a dyadic grid in the (f, Δf) plane instead of searching the whole plane to reduce the computation complexity. Before the fast kurtogram is implemented, the vibration signal is filtered by an auto-regressive filter of length of 100 to reduce transients. The first step of the fast kurtogram is to establish low-pass prototype filter $h(n)$ with cut-off frequency of $f_c = 1/8 + \varepsilon$, where $\varepsilon \geq 0$. The low-pass and high-pass filters from $h(n)$ are represented by,

$$h_l(n) = h(n)e^{j\pi n/4}, h_h(n) = h(n)e^{j3\pi n/4} \tag{4}$$

The two filtered are used to decompose the signal iteratively with each level that consists of 2^k bands. The signal from the *i*th filter is presented by $c_k^i(n)$. The filtered signal by the low-pass and high-pass filter is denoted as $c_{k+1}^{2i}(n)$ and $c_{k+1}^{2i+1}(n)$, respectively, at a decomposition level of *K-1*. The number of filtered signal is increased by a factor of 2 at each level. In addition, the respective length of signal is decreased by a factor of 2. The central frequency of the complex envelope of signal *x (n)* is represented by,

$$f_i = \left(i + 2^{-1}\right)2^{-k-1} \tag{5}$$

and the bandwidth is denoted as,

$$(\Delta f)_k = 2^{-k-1} \tag{6}$$

The kurtosis is computed for all $c_k^i(n)$ for $i = 0, ..., 2^k - 1$, $k = 0, ..., K - 1$. Based on (2), the kurtogram equals to:

$$K_k^i = \frac{\left\langle \left|c_k^i(n)\right|^4 \right\rangle}{\left\langle \left|c_k^i(n)\right|^2 \right\rangle^2} - 2 \tag{7}$$

The envelope analysis has gained popularity in bearing diagnosis because of its effectiveness and simplicity of implementation [22]. The detailed methodology is presented in reference [12, 23]. The enveloped analysis in this paper is carried on after the kurtogram by filtering the signal using a bandpass filter around the center frequency and squaring the filtered signal. The filtered signal is then low-pass filtered to obtain the envelope signal.

2.2 Sparse EWT

The empirical wavelet transform is implemented after obtaining the envelope signal from the kurtogram. The sparse EWT is composed of three parts: empirical mode decomposition, wavelet transform, and sparse representation using the l_q norm. The empirical mode decomposition (EMD) first proposed by Huang et al. [16] has enabled extraction of features of bearing vibration signals [24]. The goal of the EMD is to decompose a signal $x(t)$ into different intrinsic mode functions (IMF) and residue r as shown in (8):

$$x(t) = \sum_{i=1}^{i=n} IMF_n + r \tag{8}$$

The IMFs contains various frequency bands corresponding to different frequencies presented in the system. The calculation of the IMFs is sensitive to the signal length. As the length of the signal increases, the computation effort increases significantly. Therefore, the adaptive boundary detection method is implemented to reduce computation effort. The initial division of the boundary is specified based on the frequency of interest, which is shaft frequency and outer race fault frequency and its harmonics. A significant number of researches have demonstrated the advantage of using EMD for bearing diagnosis [25–27] and various derivations of the EMD method were proposed [19, 28]. The EWT has already demonstrated superiority in the estimation of mode and computation efficiency [29].

Wavelet transform is frequently used in signal processing of bearings to achieve the denoising of signal or extraction of features. The empirical wavelet uses the Littlewood-Paley and Meyer's wavelet shown in (9) and (10) [30]:

$$\psi(x) = (\pi x)^{-1}(\sin 2\pi x - \sin \pi x) \tag{9}$$

$$\psi_{m,n}^b(x) = 2^{-m/2}\psi(2^{-m}x - nb) \tag{10}$$

where m and n are the orthonormal basis for $L^2(\mathbb{R})$ and b is the arbitrary positive value. The assumption of the EWT separate $[0,\pi]$ into N sections. ω_n is the limit between each section (where $\omega_0 = 0$ and $\omega_N = \pi$). The empirical scaling function and the empirical wavelet are denoted by (11) and (12) [20]:

$$\phi_n(\omega) = \begin{cases} 1, if\, |\omega| \le (1-\gamma)\omega_n \\ \cos\left[\frac{\pi}{2}\beta\left(\frac{1}{2\gamma\omega_n}(|\omega| - (1-\gamma)\omega_n)\right)\right] \\ if\ (1-\gamma)\omega_n \le |\omega| \le (1+\gamma)\omega_n \\ 0,\ otherwise \end{cases} \tag{11}$$

$$\psi_n(\omega) = \begin{cases} 1, if\, (1+\gamma)\omega_n \le |\omega| \le (1-\gamma)\omega_{n+1} \\ \cos\left[\frac{\pi}{2}\beta\left(\frac{1}{2\gamma\omega_{n+1}}(|\omega| - (1-\gamma)\omega_{n+1})\right)\right] \\ if\ (1+\gamma)\omega_n \le |\omega| \le (1-\gamma)\omega_{n+1} \\ \sin\left[\frac{\pi}{2}\beta\left(\frac{1}{2\gamma\omega_n}(|\omega| - (1-\gamma)\omega_n)\right)\right] \\ if\ (1-\gamma)\omega_n \le |\omega| \le (1+\gamma)\omega_n \\ 0,\ otherwise \end{cases} \tag{12}$$

where $0 < \gamma < 1$ and $\beta(x)$ is the arbitrary function such that

$$\beta(x) = \begin{cases} 0,\ if\ x \le 0\, and\, \beta(x) + \beta(1-x) = 1\ \ \forall x \in [0,1] \\ 1,\ if\ x \ge 1 \end{cases} \tag{13}$$

The $\beta(x)$ used in this model is

$$\beta(x) = x^4\left(35 - 84x + 70x^2 - 20x^3\right) \tag{14}$$

The EWT is performed the same way as classic wavelet transform where the detail coefficients are obtained by calculating the inner products of signal with the empirical wavelets in (12). The approximation coefficients are obtained by calculating the inner products of signal with the scaling function. The reconstruction is known as (15):

$$f(t) = W_f^{\varepsilon}(0,t) \times \phi_1(t) + \sum_{n=1}^{N} W_f^{\varepsilon}(n,t) \times \psi_n(t) \tag{15}$$

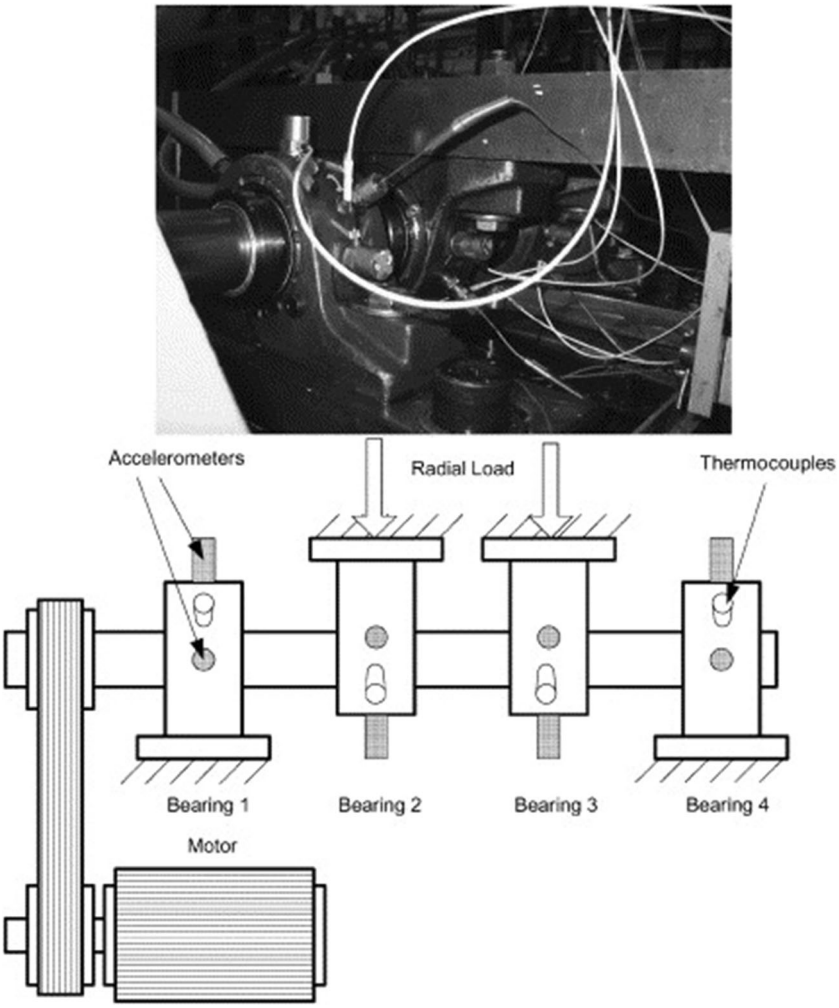

Fig. 2 Experimental setup for monitoring of bearing vibration [36]

where $W_f^{\varepsilon}(0,t)$ and $W_f^{\varepsilon}(n,t)$ are the approximation and detail coefficients, respectively, $\phi_1(t)$ is the scaling function, and $\psi_n(t)$ is the wavelet function.

Once the empirical wavelet transform is completed, the signal is reconstructed by the inverse empirical wavelet transform. Hilbert transform is performed to obtain the

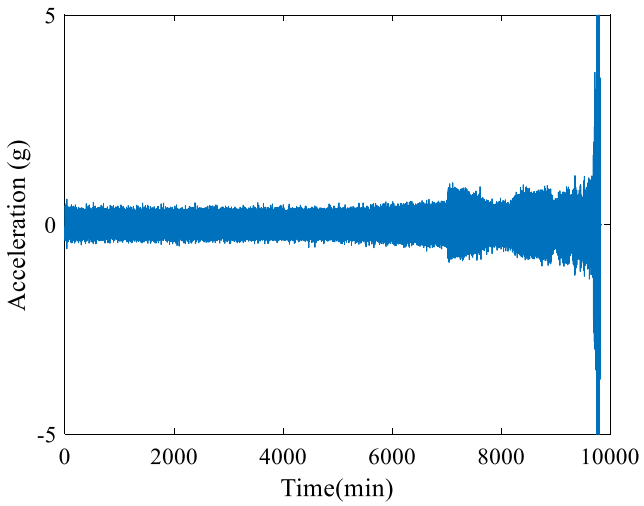

Fig. 3 Vibration signal of bearing run-to-failure test

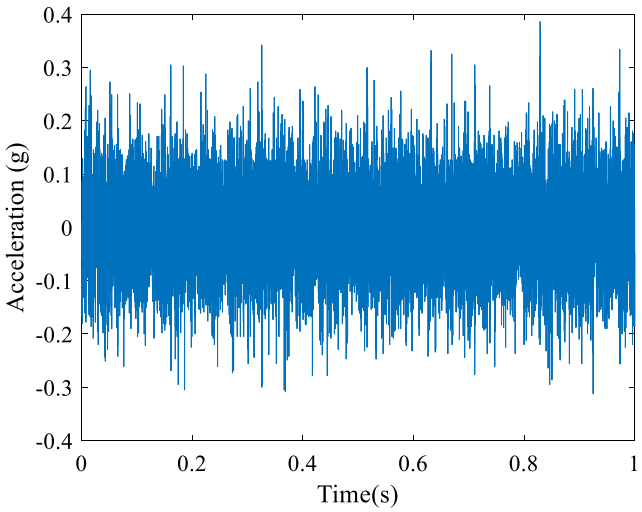

Fig. 4 Vibration signal of bearing around 4000 min

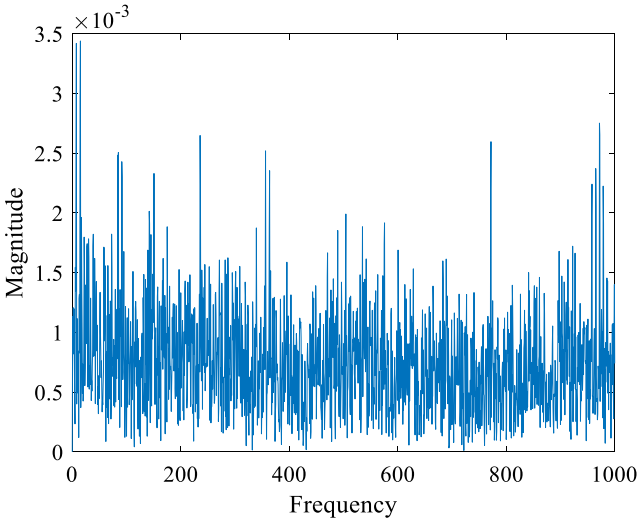

Fig. 5 Hilbert transform of unprocessed signal

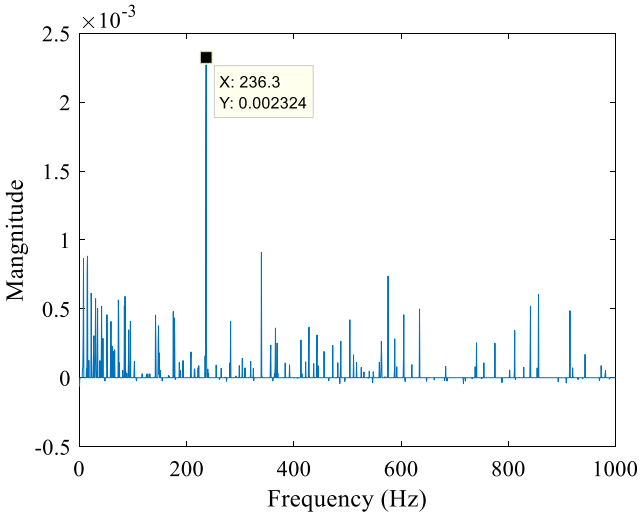

Fig. 7 Extracted fault frequency

reconstructed signal in the frequency domain. A sparse representation of the frequency domain signal is obtained to reveal the fault information. The sparsity of the empirical wavelet transform is obtained by using the l_q regularized sparse regression on the frequency domain data with $0 \le q \le 1$. The l_q regularized sparse regression solves the optimization problem:

$$\min_x \|x\|_q \; subject\ to\ y = Ax \tag{16}$$

where $x \in \mathbb{R}^m$ is the reconstructed sparse signal, $y \in \mathbb{R}^m$is the defect signal in the frequency domain and $A = 1/\sqrt{m} I_m$ with I_m as the $m \times m$ identity matrix, and $\|x\|_q = (\sum_i |x_i|^q)^{1/q}$with $0 \le q \le 1$. The l_q norm indicates that the reconstructed signal belongs to an l_q ball for $0 \le q \le 1$, which yields a sparse reconstructed signal. This soft sparsity suggests that the N most important frequencies were extracted with the error $O\left(N^{\frac{1}{2}-\frac{1}{2}}\right)$. In practice, we choose $q = 1$, which gives the Lasso, basis pursuit, or the Dantizig selector. A variety of algorithms have been developed for the l_q-regularized sparse regression, such as the l_1-based method basis pursuit [31], the Lasso [32], and the l_q-based methods [33, 34]. The theoretical analysis of the reconstruction quality can be found in reference [35] as well as references therein.

3 Experiment

To validate the proposed method, the experimental data of a bearing run-to-failure test from Qiu et al. is used [36]. The test rig for the bearings is shown in Fig. 2 with four Rexnord ZA-2115 double row bearings installed. An AC motor is used to drive the shaft at 2000 RPM. A radial load of 6000 lbs. is applied to the shaft and bearing as shown in the experimental setup. The signal from the accelerometer mounted in the horizontal direction is used. The sampling frequency is 20,480 Hz. The system is well lubricated, and a magnetic plug

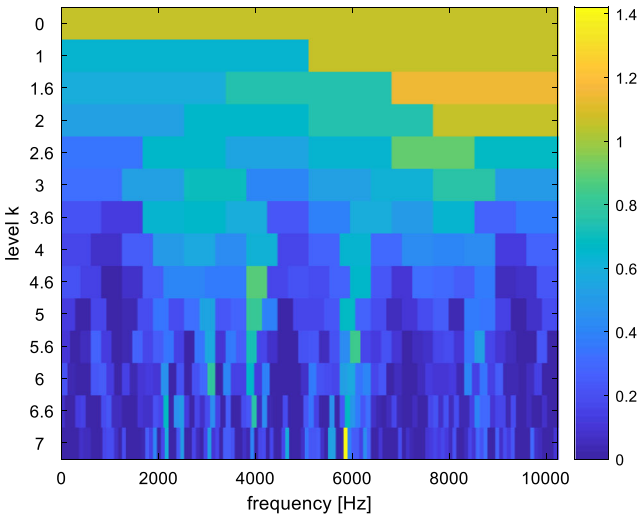

Fig. 6 Kurtogram of the weak fault signal

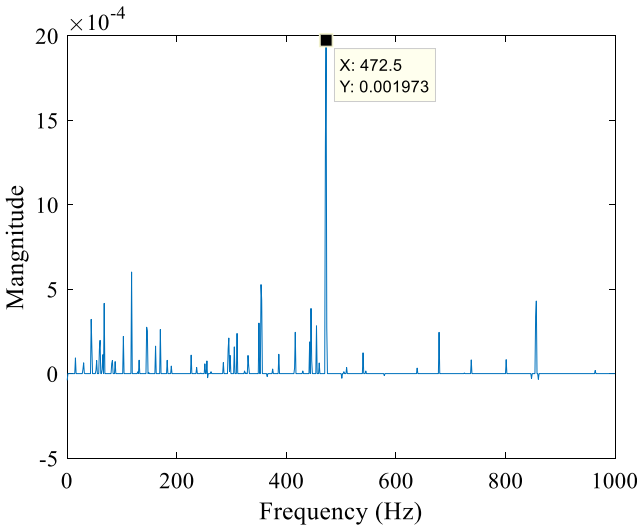

Fig. 8 Extracted harmonic of fault frequency

Table 1 Signal to noise ratio

Fault frequency	Unprocessed signal	Traditional EWT	Proposed sparse EWT
236 ± 1 Hz	0.0054	0.0101	0.1339
472 ± 1 Hz	0.0015	0.0173	0.3396

is used to collect the debris in the lubricant. Once the accumulated debris exceeds the threshold, the test will stop. The second set from the testing data is used. The failure of the outer race is observed in bearing 1 at the end of the test, and theoretical failure frequency is 236.4 Hz.

The overall vibration signal is shown in Fig. 3. To detect the early fault signature, the signal around 4000 min shown in Fig. 4 is used as weak fault signal to validate the proposed method.

4 Results

The Hilbert transform of the unprocessed signal is shown in Fig. 5. The fault signal is not distinctive in the unprocessed signal. The calculated kurtogram of the weak fault signal is shown in Fig. 6. The center frequency of the system resonance is determined to be 5880 Hz, and the bandwidth is calculated to be 80 Hz. The bandpass filter is set to keep signals within 5800 and 5960 Hz. Two different levels of the signal are filtered. The levels are selected by inspecting the kurtogram and performing principal component analysis. The obtained signals are further filtered by a 16th order Hanning window lowpass filter with the cutoff frequency equivalent to 40% of the Nyquist frequency. The filtered signal is squared to obtain the envelope signal.

The proposed sparse EWT is implemented to further enhance the signal to noise ratio of the defect signal. The extracted signal in the frequency domain calculated using the Hilbert transform is shown in Figs. 7 and 8. The signal to noise ratio is defined as the amplitude of signal at defect frequency versus all other frequencies. The corresponding signal to noise ratios of the two extracted frequencies are shown in Table 1 along with the signal to noise ratio of the unprocessed signal. The sparsity can be tuned by changing the degree of freedom of the l_q norm. In this case, a degree of freedom of 55 is chosen without sacrificing significant computation time and achieve desirable result. The traditional EWT is used as a benchmark to compare with the proposed method. It can be observed that the sparse EWT significantly reduces the random noises in the system and enhances the signal to noise ratio in Table 1.

5 Conclusions

This paper proposed a bearing diagnostic model using the kurtogram and sparse EWT to extract single weak fault signature in rolling element bearings. The model uses the kurtogram and envelope analysis for preprocessing of the signal to eliminate the transient signals and locate the frequency band of the cyclic fault. The sparse EWT further filters out undesirable noises and improves the signal to noise ratio. The proposed model demonstrates a significant improvement of signal to noise ratio in comparison with the traditional EWT model. The model has a wide range of applications in detection of early cyclic fault. By proper tuning the parameters of the kurtogram, the model is not limited to detection of single fault and its harmonics. Although the sparse EWT model yields a satisfactory result in the single fault bearing diagnosis case, the model has a few drawbacks. The proposed model is very sensitive to the Fourier boundary detection method. Different methods could yield drastic changes in the detection accuracy and computation time. The effect of the wavelet parameter has not been investigated thoroughly, which are normally chosen by default or trial and error. An optimization algorithm could be added into optimizing the wavelet parameters. Future research can be conducted to add the automatic examination feature of the kurtogram in order to implement this model in the online monitoring of the degradation process of various mechanical systems.

Author's contributions Y.L. and R.X. created the model and analyzed the data; S.Y.L. provided feedback of the concept; Y.L. and R.X. wrote the paper.

References

1. Lu Y, Li Q, Pan Z, and Liang SY (2018) Prognosis of bearing degradation using gradient variable forgetting factor RLS combined with time series model. IEEE Access
2. Liang SY, Li Y, Billington SA, Zhang C, Shiroishi J, Kurfess TR, Danyluk S (2014) Adaptive prognostics for rotary machineries. Procedia Engineering 86:852–857
3. Kurfess TR, Billington S, and Liang SY (2006) Advanced diagnostic and prognostic techniques for rolling element bearings, in Condition monitoring and control for intelligent manufacturing. Springer. p. 137–165
4. Randall RB, Antoni J (2011) Rolling element bearing diagnostics—a tutorial. Mech Syst Signal Process 25(2):485–520
5. Lu Y, Li Q, and Liang SY (2017) Adaptive prognosis of bearing degradation based on wavelet decomposition assisted ARMA model. In Technology, Networking, Electronic and Automation Control Conference (ITNEC), 2017 IEEE 2nd Information. IEEE
6. Randall RB (2011) Vibration-based condition monitoring: industrial, aerospace and automotive applications John Wiley & Sons

7. Luo H, Qiu H, Ghanime G, Hirz M, van der Merwe G (2010) Synthesized synchronous sampling technique for differential bearing damage detection. J Eng Gas Turbines Power 132(7):072501
8. Siegel D, Al-Atat H, Shauche V, Liao L, Snyder J, Lee J (2012) Novel method for rolling element bearing health assessment—a tachometer-less synchronously averaged envelope feature extraction technique. Mech Syst Signal Process 29:362–376
9. Wang Y, Xu G, Luo A, Liang L, Jiang K (2016) An online tacholess order tracking technique based on generalized demodulation for rolling bearing fault detection. J Sound Vib 367:233–249
10. Feng Z, Chen X, Wang T (2017) Time-varying demodulation analysis for rolling bearing fault diagnosis under variable speed conditions. J Sound Vib 400:71–85
11. McFadden P, Smith J (1984) Vibration monitoring of rolling element bearings by the high-frequency resonance technique—a review. Tribol Int 17(1):3–10
12. Randall RB, Antoni J, Chobsaard S (2001) The relationship between spectral correlation and envelope analysis in the diagnostics of bearing faults and other cyclostationary machine signals. Mech Syst Signal Process 15(5):945–962
13. Antoni J (2006) The spectral kurtosis: a useful tool for characterising non-stationary signals. Mech Syst Signal Process 20(2):282–307
14. Antoni J (2007) Fast computation of the kurtogram for the detection of transient faults. Mech Syst Signal Process 21(1):108–124
15. Antoni J, Randall R (2006) The spectral kurtosis: application to the vibratory surveillance and diagnostics of rotating machines. Mech Syst Signal Process 20(2):308–331
16. Huang NE, Shen Z, Long SR, Wu MC, Shih HH, Zheng Q, Yen N-C, Tung CC, and Liu HH (1998) The empirical mode decomposition and the Hilbert spectrum for nonlinear and non-stationary time series analysis. In Proceedings of the Royal Society of London A: mathematical, physical and engineering sciences. The Royal Society
17. Lei Y, Lin J, He Z, Zuo MJ (2013) A review on empirical mode decomposition in fault diagnosis of rotating machinery. Mech Syst Signal Process 35(1–2):108–126
18. Daubechies I, Lu J, Wu H-T (2011) Synchrosqueezed wavelet transforms: an empirical mode decomposition-like tool. Appl Comput Harmon Anal 30(2):243–261
19. Torres ME, Colominas MA, Schlotthauer G, and Flandrin P (2011) A complete ensemble empirical mode decomposition with adaptive noise. In Acoustics, speech and signal processing (ICASSP), 2011 IEEE international conference on. IEEE
20. Gilles J (2013) Empirical wavelet transform. IEEE Trans Signal Process 61(16):3999–4010
21. Chen J, Pan J, Li Z, Zi Y, Chen X (2016) Generator bearing fault diagnosis for wind turbine via empirical wavelet transform using measured vibration signals. Renew Energy 89:80–92
22. Borghesani P, Ricci R, Chatterton S, Pennacchi P (2013) A new procedure for using envelope analysis for rolling element bearing diagnostics in variable operating conditions. Mech Syst Signal Process 38(1):23–35
23. Antoni J (2007) Cyclic spectral analysis of rolling-element bearing signals: facts and fictions. J Sound Vib 304(3–5):497–529
24. Ali JB, Fnaiech N, Saidi L, Chebel-Morello B, Fnaiech F (2015) Application of empirical mode decomposition and artificial neural network for automatic bearing fault diagnosis based on vibration signals. Appl Acoust 89:16–27
25. Dybała J, Zimroz R (2014) Rolling bearing diagnosing method based on empirical mode decomposition of machine vibration signal. Appl Acoust 77:195–203
26. Zhang X, Zhou J (2013) Multi-fault diagnosis for rolling element bearings based on ensemble empirical mode decomposition and optimized support vector machines. Mech Syst Signal Process 41(1–2):127–140
27. Zhang J, Yan R, Gao RX, Feng Z (2010) Performance enhancement of ensemble empirical mode decomposition. Mech Syst Signal Process 24(7):2104–2123
28. Lei Y, He Z, Zi Y (2009) Application of the EEMD method to rotor fault diagnosis of rotating machinery. Mech Syst Signal Process 23(4):1327–1338
29. Kedadouche M, Thomas M, Tahan A (2016) A comparative study between empirical wavelet transforms and empirical mode decomposition methods: application to bearing defect diagnosis. Mech Syst Signal Process 81:88–107
30. Daubechies I (1992) Ten lectures on wavelets. Vol. 61 Siam
31. Chen SS, Donoho DL, Saunders MA (2001) Atomic decomposition by basis pursuit. SIAM Rev 43(1):129–159
32. Tibshirani R (1996) Regression shrinkage and selection via the lasso. JR Stat Soc Series B (Methodological):267–288
33. Li F, Xie R, Song W, Zhao T, and Marfurt K (2017) Optimal Lq norm regularization for sparse reflectivity inversion. In 2017 SEG International Exposition and Annual Meeting. Society of Exploration Geophysicists
34. Marjanovic G, Solo V (2012) On lq optimization and matrix completion. IEEE Trans Signal Process 60(11):5714–5724
35. Raskutti G, Wainwright MJ, Yu B (2011) Minimax rates of estimation for high-dimensional linear regression over lq balls. IEEE Trans Inf Theory 57(10):6976–6994
36. Qiu H, Lee J, Lin J, Yu G (2006) Wavelet filter-based weak signature detection method and its application on rolling element bearing prognostics. J Sound Vib 289(4–5):1066–1090